

# A numerical study of steady 2D flow around NACA 0015 and NACA 0012 hydrofoil with free surface using VOF method

Saadia Adjali<sup>1</sup>, Mustapha Belkadi<sup>1, a</sup>, Mohammed Aounallah<sup>1</sup>, Omar Imine<sup>2</sup>

<sup>1</sup> *Laboratory of Aero-Hydrodynamics Naval, University of Sciences and Technology of Oran-Mohamed Boudiaf, P. O. 1505El-Mnaouar Oran, Algeria.*

<sup>2</sup> *Laboratory of Aeronautics and Propulsive Systems, University of Sciences and Technology of Oran-Mohamed Boudiaf, P.O. 1505El-Mnaouar Oran, Algeria.*

**Abstract.** Accurate simulation of turbulent free surface flows around surface ships has a central role in the optimal design of such naval vessels. The flow problem to be simulated is rich in complexity and poses many modeling challenges because of the existence of breaking waves around the ship hull, and because of the interaction of the two-phase flow with the turbulent boundary layer. In this paper, our goal is to estimate the lift and drag coefficients for NACA 0012 of hydrofoil advancing in calm water under steady conditions with free surface and emerged NACA 0015. The commercial CFD software FLUENT version 14 is used for the computations in the present study. The calculated grid is established using the code computer GAMBIT 2.3.26. The shear stress  $k-\omega$ SST model is used for turbulence modeling and the volume of fluid technique is employed to simulate the free-surface motion. In this computation, the second order upwind scheme is used for discretizing the convection terms in the momentum transport equations, the Modified HRIC scheme for VOF discretisation. The results obtained compare well with the experimental data.

## 1 Introduction

Since 1960s, Computational Fluid Dynamics (CFD) has made remarkable progress. The main impetus to this progress is the increasing industrial demands. In traditional design methods, lots of model tests are required and thus it is costly and time consuming. So engineers turn to advanced numerical tools in aid of their engineering design. However, in ship industry, due to the existence of free surface and complex ship geometry, ship CFD has fallen behind the other industrial fields. But with the recent breakthrough in ship CFD technology, practical applications of CFD in analysing and predicting ship performance now become possible.

The free-surface wave induced separation is very important in ocean and marine engineering, as well as a naval architecture and offshore structures. The problem involves the complexities of free-surface deformations coupled with turbulence along with the formidable subject of three-dimensional boundary layer separations. The boundary layer analysis in the presence of the free surface becomes rather complicated due to the formation of gravity waves and the free-surface boundary condition. For instance, it is known that, for turbulent breaking waves, gravity is effective on large scale motions.

Separation due to the free-surface wave, while important in ship and platform hydrodynamics, ship performance, wake signatures and platform stability, is rather poorly understood. This paper is concerned with the wave generation due to the flow around emerged NACA 0015 and NACA 0012 moving near the free surface on 2D hydrofoil.

The Duncan (1983) experiment has been the subject of many consecutive studies. Duncan towed a fully submerged 2DNaca0012 profile at a 5° angle of attack, nose up, in steady horizontal motion. At  $Fn = 0.567$  (i.e. the wave length  $\lambda$  is equal to twice the chord length  $c$ ), when the depth  $d$  dropped below the chord length  $c$ , the first wave in the train began to break. To enhance the short range of transition in terms of the submerged depth from a breaking to a non-breaking wave train, Duncan placed a cloth ahead of the foil and towed it at foil speed for a few seconds before removing it. At critical depth disturbing the free surface resulted in a steady breaking wave train instead of the non-breaking wave train otherwise. This procedure and a more recent study, Miller (1999), confirmed the correction proposed by Banner and Phillips (1974) of the formula introduced by Stokes for the incipient breaking amplitude of a steady wave. The best we could achieve was to impose the free surface

<sup>a</sup> Corresponding author: belkadigma@yahoo.fr

measured by Duncan in a non-breaking wave train case as a slip wall condition, Laurens et al. (1999), producing the expected foil hydrodynamic coefficients and pressure contours.

Finally, this work presents the simulation results for wave formation and wave induced separation using the VOF (Volume-Of-Fluid) technique, which is a robust, free-surface modelling technique and takes the effects of air into consideration. That is, the approach solves RANS equations, simultaneously, for both water and air. In this study, the main focus is laid on the free surface wave generation for submerged hydrofoil to compute, lift and drag forces. The first study is applied to NACA 0012 hydrofoil at a 5° angle of attack for comparing the results with experimental results of Jean [1]. The second is then applied to NACA 0015 hydrofoil without free surface but at 6° angle of attack. Our study is to obtain the wave elevations, the contour of velocity magnitude and static pressure near the hydrofoil, and the values of lift and drag coefficients.

## Nomenclature

Re	Reynolds Number
$\rho$	density
$\mu$	Dynamic viscosity
g	gravity
u	x velocity
v	y velocity
w	z velocity
$\alpha_w$	volume fraction of water
$\alpha_{aa}$	volume fraction of air
$\rho_w$	density of water
$\rho_a$	density of air
$\Phi$	variable
k	turbulent kinetic energy
$\varepsilon$	Dissipation
$P_k$	production
$\mu_t$	turbulent viscosity
$\omega$	Dissipation rate
S	source
V	velocity
c	chord

## 2 Computational methods

The CFD (Computational Fluid Dynamics) results are obtained by solving RANS equations using the finite volume method. The governing equations, continuity and momentum are, as follows

$$\rho \frac{Dv_i}{Dt} = -\frac{\partial p}{\partial x_i} + \mu \nabla^2 v_i + \rho g_i, i=1, 2, 3, \quad (1)$$

$$\frac{D\rho}{Dt} + \frac{\partial v_i}{\partial x_i} = 0, \quad (2)$$

The treatment for the free-surface flow uses an interface capturing method with the Volume of Fluid (VOF). In this method, an additional transport equation is solved for the volume fraction of water in each cell. If the volume fraction of water and air in each cell is denoted as  $\alpha_w$  and  $\alpha_a$ , the tracking of the interface between the phases is accomplished by the solution of a continuity equation for the volume fraction of water. This equation has the following form:

$$\frac{\partial \alpha_w}{\partial t} + \frac{\partial}{\partial x_j} \alpha_w v_j = 0, \quad (3)$$

The volume fraction equation will not be solved for air; the volume fraction of air will be computed based on the following constraint:

$$\alpha_w + \alpha_a = 1, \quad (4)$$

The properties appearing in the transport equations are determined by the presence of the component phases in each control volume. For example, the density in each cell is given by the following:

$$\rho = \rho_w \alpha_w + \rho_a \alpha_a, \quad (5)$$

The viscosity was also computed in a similar manner.

A single momentum equation is solved throughout the domain and the resulting velocity is shared among the phases. The momentum equation is dependent on the volume fractions of all phases through the properties,  $\mu$  and  $\rho$ .

The VOF model is a fixed grid technique designed for two or more immiscible fluids where the position of the interface between the fluids is part of the unknown to be found through the solution procedure. In the VOF model, the fluids share a single set of momentum equations, and the volume fraction of each of the fluids in each computational cell is tracked throughout the domain. If the  $\alpha_w$  liquid's volume fraction in the cell noted as  $\alpha_w$ , then the following three conditions are possible:

$\alpha_w=0$ , the cell is empty (of liquid)

$\alpha_w=1$ , the cell is full (of liquid)

$0 < \alpha < 1$ , the cell contains liquid interface

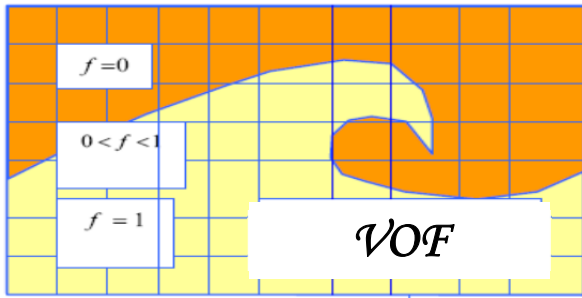


Figure 1. Advection of fluids.

Fluent has the capability to consider surface tension. The simulations were run, with and without considering surface tension, and it appeared that the surface tension had no considerable effect on the results, since other forces are considerably larger than the surface tension force.

The turbulence is modeled using the kw-SST model. The Shear-Stress Transport (SST) k- $\omega$  turbulence model is adopted to calculate eddy viscosity in our study. This model is believed to be one of the best choices to simulate turbulence flow with free surface. The governing equations of this model are as follows:

$$\frac{\partial k}{\partial t} + (U_j) \frac{\partial k}{\partial x_j} = P_k - \beta^* k \omega + \frac{\partial}{\partial x_j} \left[ \left( \nu + \frac{\nu_t}{\sigma_k} \right) \frac{\partial k}{\partial x_j} \right] + \epsilon \quad (6)$$

$$\frac{\partial \omega}{\partial t} + (U_j) \frac{\partial \omega}{\partial x_j} = \alpha \frac{\omega}{k} P_k - \beta \omega^2 + \frac{\partial}{\partial x_j} \left[ \left( \nu + \frac{\nu_t}{\sigma_\omega} \right) \frac{\partial \omega}{\partial x_j} \right] + 2 \frac{(1-F_1)}{\sigma_{\omega 2}} \frac{1}{\omega} \frac{\partial k}{\partial x_j} \frac{\partial \omega}{\partial x_j} \quad (7)$$

### 3 Test cases

#### 3.1. First case: NACA 0015

To make validation of the computational results, the simulation of the emerged NACA 0015 hydrofoil is done in the same conditions as the experiment. A hydrofoil having chord length 200 mm, speed 6 m/s, Reynolds number 1194257 and angle of attack 6° is modelled to compare the numerical results with experimental. A velocity-inlet boundary condition is applied on the upstream inflow, the velocity component is specified as 6m / s, the turbulence intensity and viscosity ratio are set as 1% and 8 respectively to specify the initial turbulence quantities. The top and bottom walls are taken as no slip walls. A simple solver is selected to solve the pressure and momentum equations, which can lead to a more robust calculation and faster convergence. The discretization schemes adopt QUICK in space, PRESTO for pressure. Figure 2 shows the structural grids generated for the NACA0015. The domain contains 112003 elements.

##### 3.1.1 Results and discussion

This section shows the effect of different turbulence models on the wetted flow results. The comparison criteria are the pressure coefficient at the stagnation point  $C_{p_{max}} = 1$ , the lift coefficient  $C_l = 2 \Pi \alpha$ , where the angle

of attack  $\alpha = 6^\circ$ , and the drag coefficient is around 0.014%  $14\% \pm$  according to the VIRTUE\_WP4 workshop report [1], there are five turbulence models provided for 2D calculations in FLUENT. It is concluded from the present study that the SST k- $\omega$  model performs better because it has smallest differences from the comparison criteria (table1).

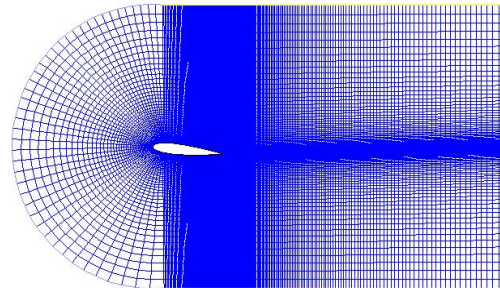


Figure 2. Computational grids for the NACA0015 foil.

Table 1. Comparison of different turbulence models

	$C_l$	Error %	$C_d$	Error %
K $\omega$ - SST	6.5729e-01	0.108 %	1.5052e-02	7.51%
K- $\omega$ Standard	6.8135e-01	3.54%	1.6009e-02	14.35%
K- $\epsilon$ Realizable	6.7966e-01	3.29%	1.4954e-02	6.814%
K- $\epsilon$	6.6500e-01	1.06%	1.6326e-02	16.61%
K- $\epsilon$ RNG	6.8529e-01	4.1%	1.5240e-02	8.85%
Criteria [1]	6.58e-01		1.40e-02	

The corresponding distributions of the pressure coefficient are represented in figure 3. From the pressure vectors along the hydrofoils, it can be observed that much larger adverse pressure occur on the pressure side of the NACA0015, this observation is also confirmed by the results of pressure coefficient distribution along our profile, as shown in figure 3. a larger separation zone is observed near the trailing edge for the NACA0015 foil, as shown in figure 4 This steeper pressure gradient also implies that more intense dynamics can be expected in the cavitating flow. A cavitation phenomenon is a complex vapor-liquid two phase flow including phase change, compressibility and viscous effects.

#### 3.2. Second case: NACA 0012 with free surface

A hydrofoil having chord length 20.3 cm, speed 0.8 m/s, Froude number 0.57, Reynolds number 1592105 and angle of attack 5° is modelled To make validation of the computational results, the simulation of the NACA 0012 hydrofoil is done in the same conditions as the experiment reported by Duncan (1983).To construct the computational domain, Gambit (Version 2.3.16) software is used. The geometry of the hydrofoil is created by using standard NACA 0012 coordinates. To mesh the two dimensional domain, it was divided into several regions in order to control the free surface and the hydrofoil

boundary layer and wake areas where structured meshes are used, whilst the rest of the domain is meshed using triangles, figure5. Hybrid meshes reduce the number of cells whilst respecting the relatively tough constrains of the solver regarding their aspect ratio and skewness, A fine meshing is applied near the free surface, The total 140000 cells are used for the computational domain. Boundary condition parameters were set with 1% turbulent intensity for the upstream flow.

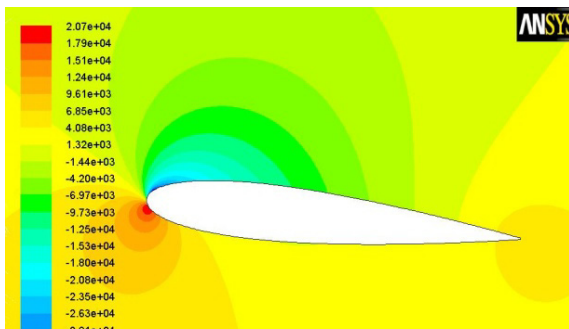
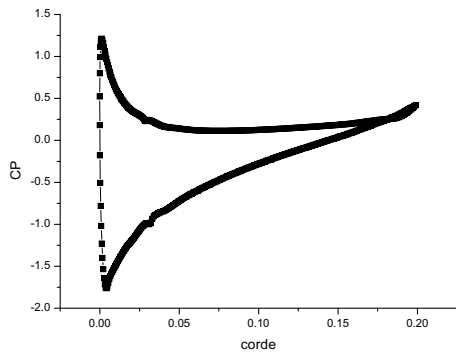


Figure 3. Pressure distribution for different grids in non-cavitating condition with SST k- $\omega$  model.

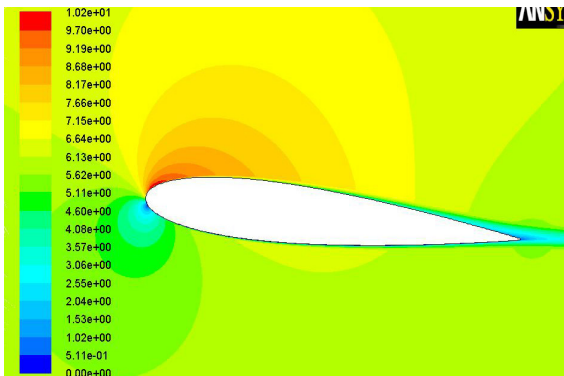


Figure 4. Contours of velocity magnitude in non-cavitating Condition with SST k- $\omega$  model

The computation domain, figure 6, was chosen large enough to be used within the range of the Froude numbers  $Fn$ . The Froude number ( $Fn = 0.57$ ) corresponds to a wave length of 0.41m ( $\lambda = 2\pi Fn^2 c$  with  $c = 203$  mm). To ensure a minimum of 2 wave lengths ahead of the hydrofoil and 4 wave lengths behind, in our domain, the bottom wall remains at a constant distance from the

hydrofoil while the position of the free surface is moved to simulate the water depth equal to 21cm.

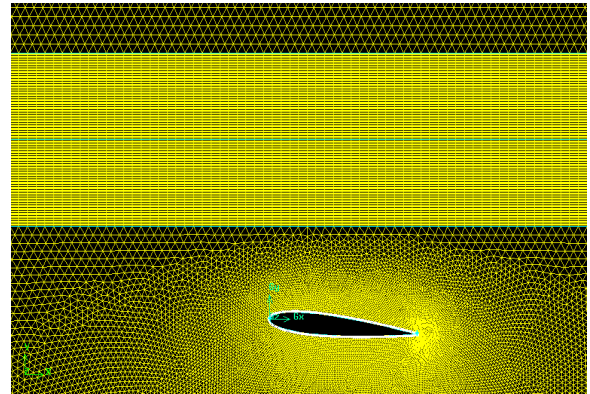


Figure 5. Mesh detail showing the hydrofoil and the free surface areas.



Figure 6. Computation domain.

To compare  $C_l$  and  $C_d$  we were adequately computed when the free surface is not present. The domain is meshed using triangles; the domain contains 133142 elements with boundary layer around profile. Mesh is shown as figure 7.

The values of the integrated forces of the NACA0012 hydrofoil without free surface predicted by FLUENT are listed in Table 2.

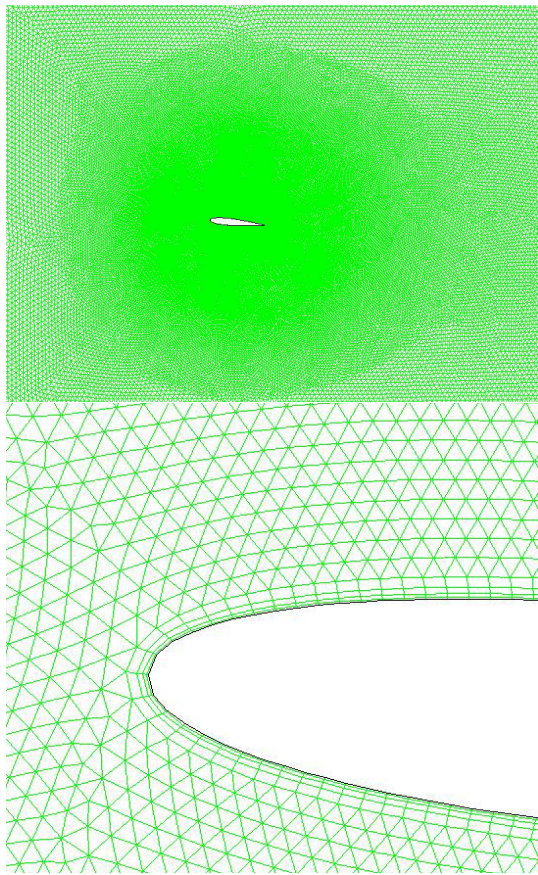
Numerical  $C_d$  and  $C_l$  obtained were respectively 0.02 and 0.48 for angle of attack  $\alpha = 5^\circ$ .

When using VOF model, the free surface is never clearly identified since between the two phases, a region of volume fraction exists as explained in the introduction, The k- $\omega$  SST k turbulence model is adopted in this study figure 7 shows the computed wave elevations along NACA 0012 for  $Fr = 0.57$ ; The maximum amplitudes of the crest is about 0.06 m, and trough of -0.07 m, and it is observed that the computed wave contains four crests and four troughs.

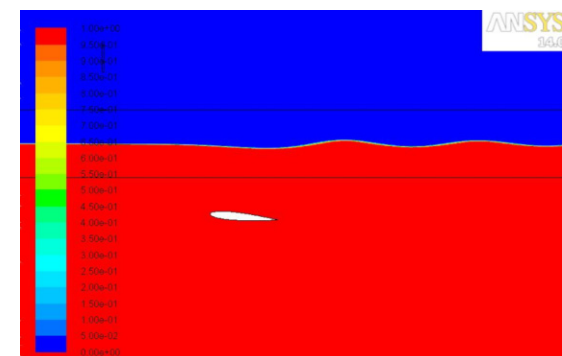
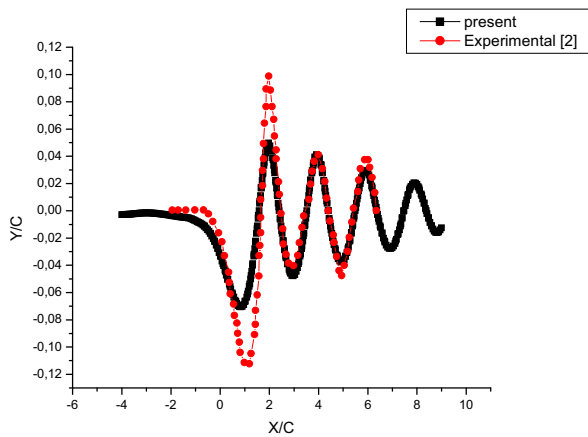
Figure 8 shows the comparison between present computational results and experimental results. From the figure it is observed that the computed wave elevations agree well with experimental wave elevations.

Table 2. Flow characteristics for NACA0012 hydrofoil

$C_l$ without free surface	$C_l$ with free surface	$C_d$ without free surface	$C_d$ with free surface
0.48	0.365	0.02	0.014



**Figure 7:** Computational grids for the NACA0012 foil, without free surface.



**Figure 8.** Wave profile along the NACA 012,  $Fr = 0.57$ .

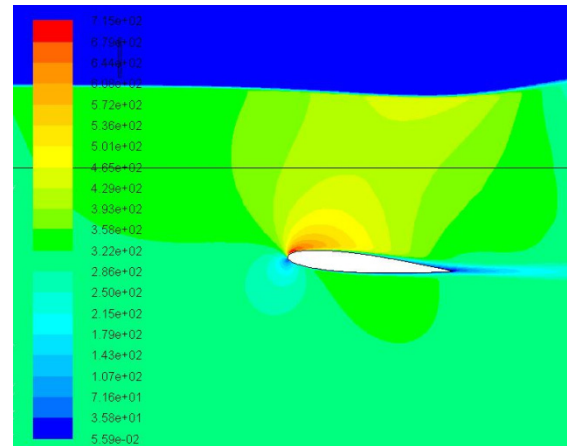


**Figure 9.** Contour of dynamic pressure around NACA 0015 hydrofoil at  $h = 21$  cm.,  $Fr = 0.57$

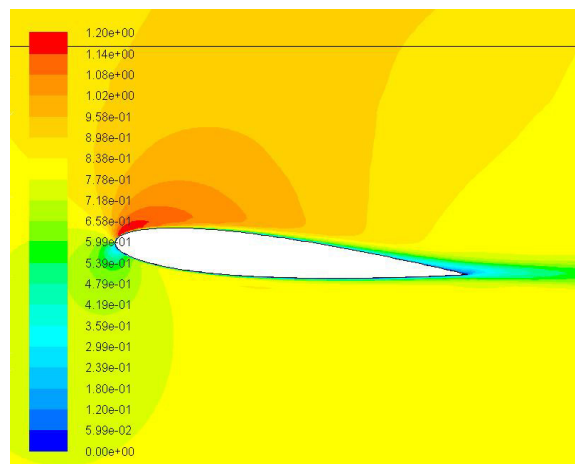


**Figure 10.** Contour of velocity magnitude around NACA 0015 hydrofoil at  $h = 21$  cm,  $Fr = 0.57$ .

Figure 9 shows the dynamic pressure around NACA 0015 hydrofoil at immersion equal to 21 cm.

In the contour of the velocity magnitude as shown in figure 10. At the leading edge and trailing edge of the hydrofoil, velocity is lower than the rest of the surface of hydrofoil.

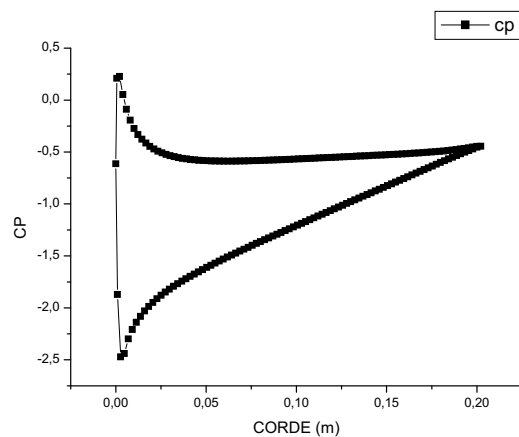


**Figure 11.** Pressure coefficient distribution along NACA 0015 condition with SST  $k \omega$  - model.

## 4 Conclusions

Computational results of a RANS model for viscous free surface flow around NACA 0012 hydrofoil and emerged NACA 0015 are presented in this paper together with a comparison of these results with experimental data. Good agreement with the experimental data has been observed.

In the present paper, implicit finite volume method (FVM) incorporating the volume of fluid (VOF) method is applied numerically to predict surface water wave caused by submerged hydrofoil moving near free surface. The  $\kappa$ - $\omega$  SST turbulence model has been implemented to capture turbulent flow around the hydrofoil in the free surface zone. From the above study, following conclusions can be drawn:

- Two-dimensional implicit finite volume method is successful for the analysis of flow around hydrofoil.
- The volume of fluid (VOF) method along with realizable  $\kappa$ - $\omega$  SST turbulence model can satisfactorily predict wave generated by the flow around hydrofoil moving near free surface.
- The present method also computes hydrodynamic forces satisfactorily.

## References

1. 1. Zi-ru Li, M Pourquie, Tom J.C. Van Terwisga, 9<sup>th</sup> International Conference on hydrodynamics of China, Shanghai, China, (2010)
2. Md. Mashud Karima, B. Prasad, b. N. Rahman, J. Ocean Engineering **78** (2014)
3. 3. J. Stigler, J. Svozil, Engineering MECHANICS, Vol. **16**, No. 6, (2009).
4. L. K. Forbes, J. Eng. Math. **19**, 329
5. LI D Q, Grekula M, Lindell P. A, Proc. of the 7th Int. Symp. On Cavitation. Ann. Arbor, Michigan, USA, (2009)
6. T. Hino, Proceedings of the 6th International Conference on Numerical Ship Hydro, Iwoa, USA. (1993)
7. G. H. Schnerr, J. Sauer, 4<sup>th</sup> Int. Conf. on Multiphase Flow. Orleans, USA, (2001).
8. Fluent Inc., FLUENT 6.3 User Guide. (2006)